Environmental Pollution 304 (2022) 119213

Contents lists available at ScienceDirect

Environmental Pollution

journal homepage: www.elsevier.com/locate/envpol

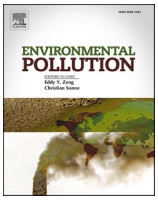

Projections of future wildfires impacts on air pollutants and air toxics in a changing climate over the western United States☆

Cheng-En Yang [a], Joshua S. Fu [a,b,*], Yongqiang Liu [c], Xinyi Dong [a,1], Yang Liu [d]

[a] Department of Civil and Environmental Engineering, University of Tennessee, Knoxville, TN, 37996, USA
[b] Computational Sciences and Engineering Division, Oak Ridge National Laboratory, Oak Ridge, TN, 37831, USA
[c] Center for Forest Disturbance Science, USDA Forest Service, Athens, GA, 30602, USA
[d] Department of Environmental Health, Emory University, Atlanta, GA, 30322, USA

ARTICLE INFO

Keywords:
Wildfires
Particulate matter
Ozone
Air toxics
Fire emissions

ABSTRACT

Wildfires emit smoke particles and gaseous pollutants that greatly aggravate air quality and cause adverse health impacts in the western US (WUS). This study evaluates how wildfire impacts on air pollutants and air toxics evolve from the present climate to the future climate under a high anthropogenic emission scenario at regional and city scales. Through employing multiple climate and chemical transport models, small changes in domain-averaged air pollutant concentrations by wildfires are simulated over WUS. However, such changes significantly increase future city-scale pollutant concentrations by up to 53 ppb for benzene, 158 ppb for formaldehyde, 655 μg/m^3 for fine particulate matter ($PM_{2.5}$), and 102 ppb for ozone, whereas that for the present climate are 104 ppb for benzene, 332 ppb for formaldehyde, 1,378 μg/m^3 for $PM_{2.5}$, and 140 ppb for ozone. Despite wildfires induce smaller changes in the future, the wildfire contribution ratios can increase by more than tenfold compared to the present climate, indicating wildfires become a more critical contributor to future air pollution in WUS. In addition, additional 6 exceedance days/year for formaldehyde and additional 3 exceedance days/year for ozone suggest increasing health impacts by wildfires in the future.

1. Introduction

Wildfires emit large amounts of particles and trace gases that can substantially influence air quality (Alves et al., 2011; Andreae and Merlet, 2001; Na and Cocker, 2008; Urbanski et al., 2008; Wiedinmyer et al., 2006). Wildfires contributed to 30% of total fine particulate matter ($PM_{2.5}$) emissions in the United States (U.S.) and carbon dioxide (CO_2) emitted from wildfires was equivalent to 4–6% of total anthropogenic emissions at the contiguous United States (CONUS) level and more than the annual emission from fossil fuel usage at the state level (Urbanski et al., 2011; Wiedinmyer and Neff, 2007). In California, U.S, 17% of the exceedances of maximum 8-h average ozone (O_3) concentrations of the U.S. public health standards were attributed to wildfires (Pfister et al., 2008). High concentrations of organic compounds after wildfires are also observed compared to that in typical urban air pollution (Alves et al., 2011; Na and Cocker, 2008). These compounds form $PM_{2.5}$, O_3, and air toxics such as benzene (BENZ) and formaldehyde (FORM) that degrade the air quality and induce adverse impacts on human health (Booze et al., 2004; Ford et al., 2018; Jaffe and Wigder, 2012; Liu et al., 2015; Reisen et al., 2015; Stowell et al., 2019).

The wildfire impacts on air pollution likely become more severe due to climate change. An increasing trend of wildfire activities in the western United States (WUS) has been observed in recent decades (Littell et al., 2009; Liu et al., 2013, 2021; Marlon et al., 2012; Wiedinmyer et al., 2006). This trend is projected to continue in the future due to more frequent fire weather conditions (e.g., reduced precipitation and soil moisture) as a result of rising global temperature (Cayan et al., 2010; Chylek et al., 2017; Gao et al., 2014; IPCC et al., 2021, 2014), leading to higher wildfire emissions. Studies have shown wildfires would enhance summertime organic carbon aerosol concentrations by 30–70% and elemental carbon concentrations by 19–27% over WUS (Spracklen et al., 2009; Yue et al., 2013), $PM_{2.5}$ by about 160%, and maximum $PM_{2.5}$ level by more than four times by the middle of the twenty-first century (Liu et al., 2016), and wildfire-related $PM_{2.5}$ in CONUS by 190% by the end

☆ This paper has been recommended for acceptance by Prof. Pavlos Kassomenos.

* Corresponding author. Department of Civil and Environmental Engineering, University of Tennessee, Knoxville, TN, 37996, USA.
E-mail address: jsfu@utk.edu (J.S. Fu).
[1] Present address: The School of Atmospheric Sciences, Nanjing University, Nanjing, Jiangsu Province, 210023, China.

https://doi.org/10.1016/j.envpol.2022.119213
Received 11 February 2022; Received in revised form 19 March 2022; Accepted 23 March 2022
Available online 27 March 2022

of the twenty-first century (Ford et al., 2018) under the Representative Concentration Pathway 8.5 (RCP8.5) emission scenario (Riahi et al., 2011).

The impacts of future wildfire emissions on air pollutant concentrations under changing climate can be better understood through improving air quality modeling and fire emission projections. Previous wildfire-related $PM_{2.5}$ and O_3 projections were based on fixed chemical lateral boundary conditions (Nolte et al., 2018), and the spatial and temporal resolutions of the air quality models were too coarse (Liu et al., 2016; Spracklen et al., 2009; Yue et al., 2013) for localized air quality management and health impact assessment purposes. One limitation with such modeling is that the air quality models often provide useful projections at regional but not city scales. In addition, BENZ and FORM, which have high health risk potentials (World Health Organization, 2010), are the most abundant non-methane volatile organic compounds (NMVOCs) emitted by fires. The lack of the projections of BENZ and FORM changes caused by wildfires can be critical to implementing air quality plans, assessing human health impacts, and improving wildland fire management strategies. Moreover, fire emissions are currently an important factor yet with the biggest uncertainty for evaluating the air quality impacts of wildfires. This problem is likely to become more crucial for evaluating future wildfire impacts since the uncertainty is expected to grow as projections of fire emissions vary dramatically with fire and fuel models (Knorr et al., 2017; Spracklen et al., 2009; Veira et al., 2016; Yue et al., 2013). The RCP8.5 emission scenario has been widely used in Earth system models for predicting climate change under an extreme anthropogenic emission scenario. This emission dataset is derived based on demographic and economic trends, technological change assumptions, and environmental legislations (Riahi et al., 2011). Although it provides gridded global pollutant emission projections (sulfur dioxide, nitrogen oxide, carbon monoxide, volatile organic compounds (VOCs), black and organic carbon aerosols), additional information is required to derive the emission of particulate matters and the grid resolution may be too coarse for city-scale air quality management purposes.

To improve the representations of fire emissions with a finer grid resolution that helps refine the projections of air quality at city scales, process-based fire models are designed to simulate the occurrence and spread of fire, fuel loading, consumption rate, and fire emissions (Liu et al., 2014a, 2021). A process-based fire model is often a part of a dynamical global vegetation model that predicts the state and change of fuel loading. It consists of several mechanistic fire behavior functions embedded in a structure that provides two-way interactions with the biogeography and biogeochemistry modules. The rates of fire spread and fireline intensity are the model estimates of fire behavior used to simulate fire occurrence. The occurrence of a fire event is triggered by thresholds of fire spread, fine fuel flammability, and coarse woody fuel moisture. Fire emissions projected by process-based fire models are also influenced by climate status expressed as varied boundary conditions of both atmospheric CO_2 and meteorological conditions such as solar radiation, temperature, humidity, and precipitation. Since fire emissions are projected on a different basis between process-based fire models and the RCP8.5 scenario, it is essential to evaluate how fire emission impacts future air pollutant concentration changes for management and decision-making on wildfires.

Through controlling the wildfire emissions, a series of regional climate and chemistry transport model simulations were conducted at high spatial and temporal resolution during the present and the future RCP8.5 climate scenarios, enabling this study to address the issues of (1) understudied BENZ and FORM projections due to wildfires, (2) the evolution of wildfire impacts on BENZ, FORM, $PM_{2.5}$, and O_3 from the past to the future at regional and city scales, and (3) uncertainty of air quality projections caused by fire emissions in WUS.

2. Material and methods

2.1. Model descriptions and model setup

Two regional models were used to evaluate wildfire impacts on air pollutant concentration changes in WUS (Fig. S1) during the present (2003–2010) and the future (2050–2059) fire months (April to November). The regional climate conditions were simulated by the Weather Research and Forecast (WRF) model (Skamarock and Klemp, 2008) version 3.2.1 that provided the meteorological information to the chemistry transport model—the Community Multiscale Air Quality (CMAQ) modeling system (Byun and Schere, 2006; Wong et al., 2012) version 5.2—to simulate the evolution of air pollutants from the present to a future climate under the RCP8.5 scenario. WRF is a state-of-the-art atmospheric model widely used for weather and regional climate research. WRF features two dynamical solvers and includes advanced numerical schemes (e.g., radiation and cloud microphysics) to realize the atmospheric processes and the interactions between atmosphere, land, and ocean. CMAQ is a comprehensive chemical transport model that consist of important processes affecting air quality and atmospheric chemistry. CMAQ uses an extensive chemical reaction database to predict the fate of chemical species through emissions and horizontal and vertical transport driven by weather conditions. In this study, both WRF and CMAQ were conducted at a high temporal (hourly) and a high horizontal (12 km × 12 km) resolution to enable the wildfire impact analyses on air pollutant concentration changes not only at regional but also at city scales. In addition to the meteorological data, CMAQ also requires the inputs of the initial and boundary conditions (ICBC) of air pollutant concentrations, and the emissions of air pollutants. A schematic diagram of the three mandatory inputs for CMAQ is shown in Fig. S2. The emission inputs are described in detail in Section 2.2 and the other two mandatory CMAQ inputs are briefly described below in this section.

We applied the dynamical downscaling technique to the three-hourly global climate model outputs (Gao et al., 2012) from the Community Earth System Model version 1, with the Community Atmosphere Model (CAM) version 4 as its atmospheric component (0.9° × 1.25° horizontal grid resolution and 26 vertical layers with the model top ~3 hPa) (Neale et al., 2010), that served as the inputs for the hourly WRF simulations during the present climate and the future RCP8.5 scenarios. Note that we used the same CAM output data as the hourly input data for WRF within three hours. The dynamically downscaled WRF results have been evaluated and demonstrated substantial improvements of the simulated meteorological conditions compared to the CAM results (Gao et al., 2012). The WRF outputs were further processed by the Meteorology-Chemistry Interface Processor (MCIP) that ingest the meteorological model output fields, transform horizontal and vertical coordinates, and prepare the meteorological fields required by CMAQ (Otte and Pleim, 2010).

The ICBC inputs of air pollutant concentrations for CMAQ were prepared using the three-hourly outputs from the global chemistry transport model integrated with the CAM model (CAM-Chem) at 0.9° × 1.25° horizontal resolution (Lamarque et al., 2012), which adopted the Model for OZone And Related chemical Tracers version 4 (MOZART4) and a bulk aerosol model (Emmons et al., 2010; Lamarque et al., 2005). MOZART4 includes an expansion of the chemical mechanism with detailed hydrocarbon chemistry and bulk aerosols to calculate several atmospheric physical and chemical processes (e.g., dry deposition and emissions of isoprene and monoterpenes). We downscaled the three-hourly CAM-Chem outputs to our study domain at 12-km horizontal resolution and assumed the air pollutant concentrations were the same within three hours. In addition, we configured CMAQ with the 2005e51 version of Carbon Bond (CB05e51) chemical mechanism (Appel et al., 2017) and the non-volatile primary organic aerosols module (Simon and Bhave, 2012) to simulate the chemical species concentrations. Species from the downscaled hourly CAM-Chem outputs

were mapped to the CMAQ CB05e51 species (Table S1) with an updated species mapping table of four VOCs due to CMAQ chemical mechanism version changes (Table S2) (Appel et al., 2017; Gao et al., 2013; Pye and Pouliot, 2012; Tai et al., 2008). Conversions of secondary organic aerosols from CAM-Chem to CMAQ were determined by the ratios between organic aerosol species in CMAQ simulations driven by the clean air ICBC (Carlton et al., 2010).

Other chemistry and physics configurations in CMAQ included the aqueous-phase chemistry module for the clouds and aqueous-phase chemistry (Fahey et al., 2017), the vertical diffusion scheme from the updated Asymmetric Convective Method (Pleim, 2007), the horizontal advection scheme (Colella and Woodward, 1984), inline photolysis rate calculations (Binkowski et al., 2007), inline lightning induced nitrogen oxides (Allen et al., 2010, 2012), and inline plume-rise modules for emissions (UNC Institute for the Environment, 2009).

2.2. Emissions

2.2.1. Present years emissions

The emissions of air pollutants are critical CMAQ inputs to assess how their concentrations vary with wildfires under climate change. The present emissions obtained from the U.S. Environmental Protection Agency (USEPA) were derived from the National Emission Inventory data (Xing et al., 2013). These emissions include point, mobile, and area emission sources during 2001–2010 over the CONUS domain (Fig. S1). The point sources comprise anthropogenic emissions from electric generating units, non-electric generating units, and other point sources outside CONUS (i.e., Canada, Mexico, and near-coast oceans). The mobile sources include on-road and non-road vehicle emissions. The area sources consist of anthropogenic emission sectors (e.g., industrial processes, solvent, and agricultural production) and biogenic emissions at the surface at 36-km horizontal resolution. We processed the area emissions by regridding it to the 12-km horizontal resolution based on the 2000–2010 U.S. population data at the county level (https://www.census.gov/data/tables/time-series/demo/popest/intercensal-2000-2010-counties.html).

The present fire emissions were prepared utilizing two fire emission products—Fire INventory version 1.5 from National Center for Atmospheric Research (FINN) (Wiedinmyer et al., 2011) and Global Fire Emissions Database version 4.1 with small fires (GFED4.1s) (Giglio et al., 2013)—to reconstruct the fire emissions that were aggregated into the USEPA area source emissions (Fig. S2). FINN data contains 40 daily fire-induced species emissions from satellite retrievals at about 1-km horizontal resolution using the MOZART4 chemical mechanism. Chemical species in FINN were mapped to the CB05e51 species accordingly (Tables S1 and S2). The GFED4.1s dataset provides the fire activity information every three hours at 0.25° horizontal resolution starting from 2003. We applied the nearest neighbor method to reallocate the daily FINN emissions with the three-hourly GFED4.1s temporal profiles for generating the hourly FINN emissions. Note that the FINN emission rate of a species in a grid cell was assumed the same within three hours. We further distributed hourly FINN fire emissions vertically with the hourly meteorological conditions from WRF and the GFED4.1s burned area sizes according to the injection height of biomass burning emission (Fu et al., 2012), along with the hourly buoyant efficiency and the fire size class look up tables (Tables S3 and S4) (Air Sciences Inc, 2005). The resulting three-dimensional hourly FINN emissions (FINN3D) were used for the 2003–2010 simulations due to the GFED4.1s data availability limitation. We adjusted the area emissions by subtracting the surface layer data in FINN3D from the USEPA area source data and zeroed out the grid cells with negative values.

2.2.2. Future emissions

Future emissions under the RCP8.5 scenario were prepared with the data from the International Institute for Applied Systems Analysis (IIASA) database (available at https://tntcat.iiasa.ac.at/RcpDb). This database provides twelve sectoral emissions at 0.5° horizontal resolution on a monthly basis in 2000, 2005, and every decade from 2010 to 2100. To obtain 2051–2059 emissions, we firstly interpolated the emissions between 2050 and 2060 linearly and mapped the twelve IIASA emission sectors to the five emission source types used in the present years emissions (Table S5). The eight species of IIASA emissions were also mapped to the CB05e51 species (Table S6). We then computed the monthly ratios of all species at each grid cell in each IIASA emission source between 2050s and 2005, and these ratios were applied to the corresponding 2005 USEPA emission source types and the 2005 FINN3D fire emissions, yielding the projected 2050–2059 hourly emissions for wildfires (FINN3D_RCP85) and all the other sectors. Note that we chose 2005 as the base year to project future emissions because the historical period ended in 2005 for the climate model simulations in the fifth phase of the Coupled Model Intercomparison Project (Taylor et al., 2012). In addition, the same ratio of a species at a grid cell in monthly IIASA emissions was applied to the 2005 hourly USEPA emission data of that species within a month, i.e., a species would have the same spatial and temporal emission distributions at a grid cell as it had in 2005 but with a different magnitude within a month. Furthermore, we assumed the future biogenic emissions would have the same emission ratios derived from the IIASA anthropogenic emissions because both emissions were already merged into the USEPA area source emissions.

2.2.3. Future fire emissions from a process-based fire model

The FINN3D_RCP85 fire dataset was derived from the spatial and temporal profiles of FINN3D with the magnitudes from the 2050s to 2005 IIASA emission ratios. Since the global IIASA emissions have a coarser grid resolution, we used a process-based empirical fire model (EFM) to project fire emissions with a finer grid resolution for CMAQ simulations. In this study, we compared the simulated air pollutant concentrations between FINN3D_RCP85 and EFM to evaluate how fire emissions impact the air pollution in WUS.

EFM is a fire model based on the extreme value theory and fuel projection of a dynamic global vegetation model (Liu et al., 2014b, 2021). It requires fire danger meteorological variables (daily maximum temperature and precipitation, annual mean precipitation, and humidity), which can be obtained from observations or from climate and weather modeling results, as the inputs to predict the average fire number over different fire size ranges and various levels of a normalized drought index (Liu et al., 2021). The ratio of the projected fire numbers to that in the present years for each fire size category is applied to the burned area from observations at the present years to estimate the future burned area for the category. The fire projection information, along with the fuel loading predicted by the Dynamical Land Ecosystem Model (Tian et al., 2010) and the fuel moisture calculated by the empirical algorithms from the National Fire Danger Rating System (Cohen and Deeming, 1985), can be used to project future $PM_{2.5}$ emissions from wildfires (Liu et al., 2021). In this study, we estimated future EFM emissions at the locations where large fires (at least 1,000 acres burned) occurred during 2003–2010 and the $PM_{2.5}$ emissions from large fires in WUS were projected to increase during 2050–2059 (Fig. S3). The major contributor is the increasing number of large fires, which would lead to an increase of total $PM_{2.5}$ emissions by about 50% by the middle of the twenty first century; changes in fuel loading would also contribute to the increase in $PM_{2.5}$ emissions, but with large spatial variability (Liu et al., 2021). We prepared the EFM emissions through aggregating the $PM_{2.5}$ emissions located within a 12-km grid cell over WUS, and we applied the emission factor ratios based on Urbanski et al., 2014 for each species to $PM_{2.5}$ (Table S7) to derive the emissions of other species from wildfires.

2.3. Experimental design and analytical metrics

Two sets of hourly CMAQ simulations with five different emission scenarios were conducted to investigate the wildfire impacts on the air pollutants from the present to the future climate (Table S8). The first

simulation set includes two present climate experiments of EXP1 (without fire emissions) and EXP2 (with FINN3D emissions) during 2003–2010 under the same meteorological conditions and ICBC values. The second simulation set includes three experiments under the RCP8.5 scenario. These three experiments share the same future year WRF inputs, ICBC inputs, and sectoral emissions except for wildfires. EXP3 was conducted excluding wildfire emissions, EXP4 with the FINN3D_RCP85 emissions, and EXP5 with the EFM emissions.

In this study, we evaluate the wildfire impacts on four air pollutants (BENZ, FORM, $PM_{2.5}$, and O_3) each fire month, with the daily averages of $PM_{2.5}$ and the hourly values of the other pollutants. The analytical metrics include the grid-cell level (or "city-scale") values and the domain averages of all grid-cell values, the differences of the grid-cell level values and the domain averages between with and without wildfire emission experiments, and the wildfire contribution ratios at the grid-cell level (R_{grid}) and the domain averages (R_{avg}):

$$R_{grid} = \left(\frac{EXP_{fire} - EXP_{nofire}}{EXP_{nofire}}\right)_{grid}, \quad (1)$$

$$R_{avg} = \overline{\left[\frac{(EXP_{fire} - EXP_{nofire})_{grid}}{(EXP_{nofire})_{grid}}\right]}, \quad (2)$$

where EXP_{fire} is EXP2 for the present climate and EXP4 or EXP5 for the future climate. EXP_{nofire} is EXP1 for the present climate and EXP3 for the future climate. A recent study has shown that long-term exposure to air pollutants induces adverse health effects even at low concentration levels (Dominici et al., 2022). Hence, compared to the fire contribution percentages used in previous studies (e.g., Liu et al., 2016; Wilkins et al., 2018), R_{grid} and R_{avg} can better illustrate how wildfires aggravate air quality on top of an environment without wildfires, especially at lower pollutant concentration levels. In addition, we calculate the number of exceedance days at the grid-cell level according to the National Ambient Air Quality Standards and the reference exposure levels (REL) (OEHHA, 2008) to investigate the wildfire impacts on air quality. We define an exceedance day of a species as the daily averaged value reaches or exceeds its threshold (for $PM_{2.5}$ only) or any hourly value within a day reaches or exceeds its threshold (for O_3, BENZ, and FORM). In this study, we adopt the threshold values of 35 μg/m^3 for daily $PM_{2.5}$ and 70 ppb for hourly O_3 (National Primary and Secondary Ambient Air Quality Standards, 2021), and the acute REL values of 27 μg/m^3 (or 8.5 ppb) for hourly BENZ and 55 μg/m^3 (or 45 ppb) for hourly FORM (OEHHA, 2008).

The CMAQ performance was assessed retrospectively during the present climate through pairing modeled outputs and observations in time and in space. We used the mean fractional bias and the mean fractional error metrics (Boylan and Russell, 2006) to evaluate the simulated daily $PM_{2.5}$ and hourly O_3 concentrations in WUS. We retrieved monitoring station data from the Interagency Monitoring of Protected Visual Environments database (available at http://vista.cira.colostate.edu/Improve/improve-data) and the Air Quality System (available at https://aqs.epa.gov/aqsweb/airdata/download_files.html) in WUS during the 2003–2010 fire months. All data from monitoring sites within a model grid cell was averaged and compared to the modeled values. We verified that the EXP2 results meet the performance goal for hourly O_3 values excluding data points smaller than 40 ppb and the performance criteria for daily $PM_{2.5}$ (Table S9), validating the feasibility of our CMAQ configurations and inputs for projecting wildfire impacts on air pollutant concentrations in WUS.

3. Results and discussion

3.1. Wildfire impacts on air toxics in WUS

The monthly domain-averaged BENZ concentrations without wildfire emissions decrease from 0.014 to 0.039 ppb in EXP1 during the present climate to 0.009–0.023 ppb in EXP3 under the RCP8.5 scenario (Fig. 1(a)). With the consideration of wildfire emissions, such values change to 0.016–0.050 ppb for EXP2, 0.012–0.045 ppb for EXP4, and 0.009–0.023 ppb for EXP5, respectively. The yielding differences caused by wildfires are 0.001–0.025 ppb during the present climate and enhance to 0.002–0.027 ppb in the 2050s with the FINN3D_RCP85 emissions. Compared to EXP3, the domain-averaged BENZ concentrations in EXP5 show small changes with the EFM emissions in the 2050s. Contrary to the small changes of domain-averaged concentrations, the monthly maximum BENZ levels and the enhancement of BENZ concentrations by wildfires are simulated much higher at the grid-cell level (Fig. 1(b)). The monthly maximum BENZ concentrations at the grid-cell level are 3–8 ppb in EXP1 and 5–104 ppb in EXP2, with the differences ranging 5–104 ppb in the present climate. During the 2050s, the maximum BENZ concentrations at the grid-cell level are projected 2–7 ppb in EXP3, 7–53 ppb in EXP4, and 0.001–30 ppb in EXP5. The future BENZ increases by wildfires are simulated up to 53 ppb with the FINN3D_RCP85 emissions and up to 30 ppb with the EFM emissions. Our results indicate that fire emissions can substantially worsen the air quality at cities in WUS despite the insignificant contributions to the entire WUS domain. Note that our simulated BENZ concentrations with wildfire emissions in the present climate are higher than previous measured 3–4 ppb in WUS (Reinhardt and Ottmar, 2004), primarily attributed to larger burned areas under climate change such as summertime precipitation declines and exacerbated vapor pressure deficits (Dennison et al., 2014; Higuera and Abatzoglou, 2021; Holden et al., 2018; Short, 2013).

The monthly domain-averaged FORM concentrations are 0.33–0.87 ppb in EXP1 and 0.33–0.92 ppb in EXP2 during the present climate. Relatively lower FORM concentrations are projected under the RCP8.5 scenario, with 0.27–0.73 ppb in EXP3 excluding wildfire emissions, 0.28–0.75 ppb in EXP4 with the FINN3D_RCP85 emissions, and 0.27–0.73 ppb in EXP5 with the EFM emissions, respectively (Fig. 2(a)). Wildfires enhance FORM concentrations by 0.003–0.048 ppb during the present climate and 0.006–0.040 ppb in the 2050s with the FINN3D_RCP85 emissions. Similar to BENZ, EXP5 with the EFM emissions exhibits no substantial FORM concentration changes compared to EXP3 at the regional scale (Fig. 2(a)). On the contrary, the maximum differences of FORM concentrations at the grid-cell level can be as high as 82 ppb (Fig. 2(b)), which is nearly doubled than the suggested REL

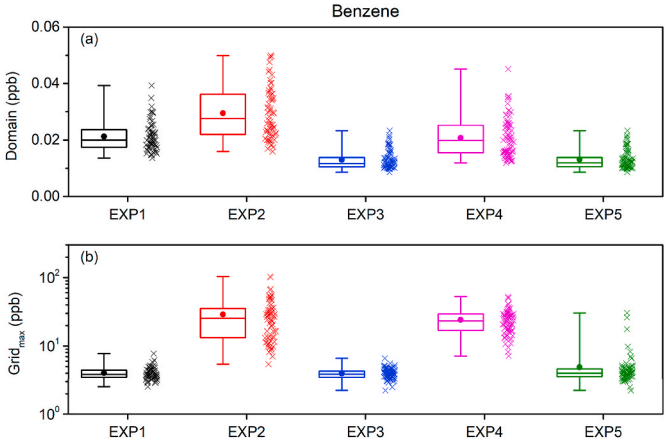

Fig. 1. Monthly (a) domain-averaged and (b) grid maximum benzene concentrations (cross marks, unit: ppb) in WUS. The definitions of experiments are described in the main texts. Each box-whisker plot includes the information of the minimum (lower end), the first quartile (lower bound of the box), the median (line inside the box), the third quartile (upper bound of the box), and the maximum (upper end). Mean values are shown in filled circles. Note the ordinate is in log-scale in panel (b).

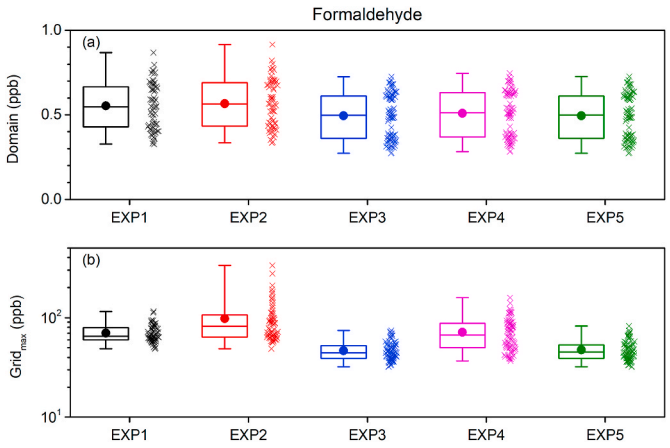

Fig. 2. Monthly (a) domain-averaged and (b) grid maximum formaldehyde concentrations (cross marks, unit: ppb) in WUS. The definitions of experiments are described in the main texts. Each box-whisker plot includes the information of the minimum (lower end), the first quartile (lower bound of the box), the median (line inside the box), the third quartile (upper bound of the box), and the maximum (upper end). Mean values are shown in filled circles. Note the ordinate is in log-scale in panel (b).

threshold of FORM. The monthly maximum FORM concentrations at the grid-cell level are 49–116 ppb in EXP1 and 49–333 ppb in EXP2, with the differences ranging 15–332 ppb in the present climate. Our simulated FORM concentrations in 2003–2010 are much higher than previously measured 6–13 ppb in WUS during 1992–1995 (Reinhardt and Ottmar, 2004) and 2–11 ppb over California in 2003 (Na and Cocker, 2008) during wildfire events. It is suggested that more intensified fire activities during 2003–2010 as a result of a drier environment with exacerbated vapor pressure deficits (Dennison et al., 2014; Higuera and Abatzoglou, 2021). The projected monthly maximum FORM concentrations at the grid-cell level are 32–74 ppb in EXP3 and 37–159 ppb in EXP4, resulting in 19–158 ppb increases by the FINN3D_RCP85 emissions.

The simulated BENZ and FORM concentrations in the 2050s are lower than that in the present climate, which are associated with the anthropogenic NMVOCs emission reductions as a result of future technological improvements (Myhre et al., 2013; Riahi et al., 2011). Instead of smaller increases in BENZ and FORM, wildfires can induce higher contribution ratios in the future than that in the present climate, implying a more vital role of future wildfires in enhancing BENZ and FORM concentrations. During 2003–2010, the largest monthly domain-averaged BENZ increase by wildfires is simulated 0.025 ppb in August 2003, which is 23% of the total BENZ with 1.67 for R_{avg} (Fig. S4); the domain-averaged FORM increase by wildfires is simulated 0.048 ppb the greatest in August 2007, that is 2% of the total FORM and 0.06 for R_{avg} (Fig. S5). In the 2050s, the domain-averaged BENZ increase utilizing the FINN3D_RCP85 emissions is only 0.007 ppb in April 2058 and 17% for the contribution percentage while R_{avg} increases to 2.2 (Fig. S4); the domain-averaged FORM increase is projected 0.04 ppb in October 2054, contributing to 4% of the total FORM whereas R_{avg} becomes 0.11 (Fig. S5). Results from EXP5 show that the EFM emissions have much smaller impacts on domain-averaged BENZ (up to 6×10^{-4} ppb changes and 0.11 for R_{avg}) and FORM (up to 10^{-3} ppb changes and 3×10^{-3} for R_{avg}) in WUS than EXP4 with the FINN3D_RCP85 emissions (Figs. S4 and S5), yet significant changes are simulated at the grid-cell level. The largest wildfire impact of EXP5 with respect to EXP3 at the grid-cell level are found 30 ppb for BENZ and 82 ppb for FORM in October 2052, while the highest R_{grid} values are 7,066 for BENZ and 264 for FORM in August 2055 (Figs. S6 and S7). The greatest wildfire-induced changes at the grid-cell level during the present climate are simulated 104 ppb in October 2008 for BENZ and 332 ppb for FORM in September 2006, and the maximum R_{grid} values are found 2×10^7 for BENZ in May 2009 and 1×10^3 for FORM in November 2003. For the FINN3D_RCP85 emissions under the RCP8.5 scenario, wildfires enhance BENZ by up to 53 ppb in August 2053 and up to 158 ppb for FORM in August 2051, with the maximum R_{grid} values of 5×10^6 for BENZ in April 2050 and 1×10^3 for FORM in November 2052. It is noteworthy that the highest domain-averaged values and grid-cell maximum values of BENZ and FORM are simulated in different months between the present climate and the future climate. This result elucidates the importance of climate change to the evolution of wildfire impacts on the air toxics in WUS, which is crucial to the decision-making strategies for fire and environmental management since high air toxics levels are not only simulated in summertime but also during the spring and autumn seasons in the future (Figs. S5–S7).

The high R_{grid} values simulated under the RCP8.5 scenario suggest that cities in WUS will experience substantial BENZ and FORM increases when wildfires take place, in spite of reduced concentrations and contribution percentages, which may impose threat to the sensitive groups. To better illustrate the air quality changes and health impacts by wildfires, we evaluate the annual exceedance days across the WUS domain. The exceedance days for BENZ rise by 41% (100 days/year) due to wildfires during the present climate while that during the 2050s are 39% (95 days/year) for EXP4 (Table 1). Nevertheless, the exceedance days for FORM increase from 34% (84 days/year) to 44% (108 days/year) in the present climate while that for EXP4 surges by 12% (30 days/year) to 19% (47 days/year). Fewer exceedance days for EXP4 than EXP2 but with greater changes when compared to no wildfire emission scenarios suggest that wildfires become much more important regarding air quality in the future. The exceedance days for both BENZ and FORM in EXP5 only increase by 1 day/year (Table 1), which are fewer than EXP4 because the EFM emissions only consider large wildfires while the FINN3D_RCP85 emissions take both large and small wildfires into account.

3.2. *Wildfire impacts on $PM_{2.5}$ and O_3*

Wildfires elevate the monthly domain-averaged $PM_{2.5}$ from 2.56 to 8.04 μg/m^3 to 2.63–9.30 μg/m^3 in WUS during the present climate (Fig. 3(a)), causing 0.05–1.26 μg/m^3 increases in $PM_{2.5}$. The maximum change is simulated in August 2007, the largest R_{avg} of 0.20 in September 2006, and the highest contribution percentage of 9% in July 2008 (Fig. S8). Our results are slightly lower than previous studies that estimated wildfires-induced $PM_{2.5}$ increases of 1.48 μg/m^3 with a contribution ratio of 11% at the Intermountain West region in June–September during 2008–2012 (Wilkins et al., 2018), and on an average 12% of total daily $PM_{2.5}$ at 561 counties in WUS during 2004–2009 (Liu et al., 2016). A longer fire season (April to November) and a broader domain with more states included in our analysis are

Table 1
Exceedance days per year and percentages (%) during the fire months (April–November) in WUS. The O_3 values exclude data less than 40 ppb. An exceedance day is defined as any grid cell within the WUS domain exceeds the threshold value of a pollutant in a day.

Time period	Experiment	Pollutants			
		BENZ	FORM	$PM_{2.5}$	O_3
Present (2003–2010)	EXP1	0 (0%)	84 (34%)	39 (16%)	208 (85%)
	EXP2	100 (41%)	108 (44%)	182 (75%)	210 (86%)
Future RCP8.5 (2050–2059)	EXP3	0 (0%)	17 (7%)	52 (21%)	194 (80%)
	EXP4	95 (39%)	47 (19%)	174 (71%)	199 (82%)
	EXP5	1 (0%)	18 (7%)	55 (23%)	194 (80%)

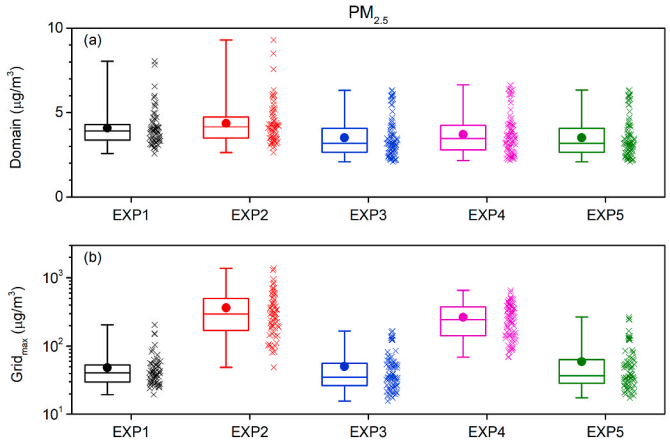

Fig. 3. Monthly (a) domain-averaged and (b) grid maximum $PM_{2.5}$ concentrations (cross marks, unit: μg/m^3) in WUS. The definitions of experiments are described in the main texts. Each box-whisker plot includes the information of the minimum (lower end), the first quartile (lower bound of the box), the median (line inside the box), the third quartile (upper bound of the box), and the maximum (upper end). Mean values are shown in filled circles. Note the ordinate is in log-scale in panel (b).

suggested to cause the lower wildfire impacts on $PM_{2.5}$ in this study. In addition, our results demonstrate that wildfires slightly enhance $PM_{2.5}$ concentrations more in the autumn seasons (0.17–0.93 μg/m^3, R_{avg} = 0.05–0.20, contribution percentages = 3–8%) with an average of 0.36 μg/m^3 than in the summer seasons (0.05–1.26 μg/m^3, R_{avg} = 0.01–0.18, contribution percentages = 1–9%) with an average of 0.34 μg/m^3 during the present climate (Fig. S8). While studies have shown large wildfire impacts on summertime $PM_{2.5}$ concentrations in WUS (Jaffe et al., 2008; O'Dell et al., 2019), the shift of higher wildfire impacts on $PM_{2.5}$ from summer to autumn seasons simulated in this study is associated with the enhanced wildfire activities under climate change, driven by the heightened fire vulnerability as a result of altered temperature, wind, and precipitation patterns in WUS (Goss et al., 2020; Williams et al., 2019). At city scales, the maximum wildfire-induced $PM_{2.5}$ change is found 1,378 μg/m^3 in September 2006, which is 767 times higher than the $PM_{2.5}$ level if there were no wildfires (Fig. S9). During 2003–2010, wildfires increase 47–1,378 μg/m^3 at city scales, resulting in 21–767 for R_{grid} and 95–100% for the wildfire contribution percentages. The autumn seasons are influenced by wildfires (194–1,378 μg/m^3, R_{grid} = 69–797) much greater than the summer seasons (76–948 μg/m^3, R_{grid} = 29–302) (Fig. S9).

The domain-averaged $PM_{2.5}$ projections under the RCP8.5 scenario range 2.08–6.32 μg/m^3 in EXP3, 2.16–6.64 μg/m^3 in EXP4, and 2.08–6.33 μg/m^3 in EXP5, whereas $PM_{2.5}$ levels at city scales are simulated 17.4–38.1 μg/m^3 in EXP3, 91.0–260.6 μg/m^3 in EXP4, and 17.4–38.1 μg/m^3 in EXP5 (Fig. 3(a)). The resulting domain-averaged $PM_{2.5}$ changes by wildfires are 0.06–0.70 μg/m^3 (R_{avg} = 0.03–0.20, contribution percentages = 2–9%) with the FINN3D_RCP85 emissions and up to 0.03 μg/m^3 (R_{avg} = 0.01, contribution percentages = 0.5%) with the EFM emissions (Fig. S8); the grid-cell level maximum $PM_{2.5}$ changes are 67–655 μg/m^3 (R_{grid} = 34–271, contribution percentages = 97.1–99.6%) with the FINN3D_RCP85 emissions and 0.1–265 μg/m^3 (R_{grid} = 0.03–90.4, contribution percentages = 2.7–98.9%) with the EFM emissions (Fig. S9). The projections of domain-averaged and grid-cell level $PM_{2.5}$ concentrations in the 2050s are smaller than the present climate (Fig. 3), consistent with the projected BENZ and FORM results, caused by anthropogenic emission reductions with improved technologies in the future (Ford et al., 2018; Riahi et al., 2011; Val Martin et al., 2015). Although the changes are smaller in the future, the slightly higher R_{avg} values indicate an increasing importance role of wildfires in future $PM_{2.5}$ across the WUS domain as suggested by previous studies (Ford et al., 2018; Liu et al., 2016). The large R_{grid} values in both simulations with the FINN3D_RCP85 emissions and the EFM emissions also suggest substantial wildfire contributions on local $PM_{2.5}$ that can induce health concerns. Our simulations show that the $PM_{2.5}$ exceedance days caused by wildfires are 143 days/year (59%) in the present climate and 122 days/year (50%) with the FINN3D_RCP85 emissions and 3 days/-year (2%) with the EFM emissions under the RCP8.5 scenario (Table 1).

The monthly domain-averaged O_3 levels between EXP1 and EXP2 are close each other during the present climate (Fig. 4(a)). The differences caused by wildfires are simulated 0.03–0.62 ppb (R_{avg} = 0.001–0.012, contribution percentages = 0.06–1.14%) (Fig. S10), which are comparable to the previously reported value of 0.17 ppb or 0.4% for maximum 8-h average O_3 increases across the CONUS domain during the 2008–2012 fire seasons (Wilkins et al., 2018). The city-scale maximum O_3 changes are projected 9.8–139.6 ppb (R_{grid} = 0.2–3.4, contribution percentages = 20–78%) with the largest values simulated in June 2008 (Fig. S11). Compared to the higher impacts during the autumn seasons for $PM_{2.5}$, summertime wildfires influence O_3 changes the most in WUS for both the domain-averaged (0.08–0.62 ppb, R_{avg} = 0.002–0.012, contribution percentages = 0.16–1.14%) and city-scale maximum O_3 values (23.8–139.6 ppb, R_{grid} = 0.5–3.4, contribution percentages = 34–78%).

Future monthly domain-averaged and city-scale maximum O_3 concentrations are simulated higher under the RCP8.5 climate than that of the present climate (Fig. 4). The domain-averaged values are 46.5–54.9 ppb in EXP3, 46.6–54.9 ppb in EXP4, and 46.5–54.9 ppb in EXP5. The O_3 increases induced by wildfires are up to 0.24 ppb (R_{avg} = 0.005, contribution percentage = 0.5%) with the FINN3D_RCP85 emissions and up to 0.01 ppb ($R_{avg} = 1 \times 10^{-4}$, contribution percentages = 0.01%) with the EFM emissions (Fig. S10). Summer remains the most influential season for O_3 increases by wildfires in WUS during the 2050s, consistent with previous studies, as a result of enhanced fire activities and increased biogenic emissions under a warmer climate condition (e.g., Jaffe and Zhang, 2017; Nolte et al., 2018). The maximum O_3 values at the grid-cell level increase by wildfires are 6.2–102.5 ppb (R_{grid} = 0.1–2.3, contribution percentages = 13–70%) for all fire months and 19.3–102.5 ppb (R_{grid} = 0.4–2.3, contribution percentages = 29–70%) during the summer seasons with the FINN3D_RCP85 emissions. Simulations with the EFM emissions show 0.01–42.3 ppb ($R_{grid} = 3 \times 10^{-4}$–1.03, contribution percentages = 0.03–50.6%) for all fire months and 0.1–42.3 ppb (R_{grid} = 0.002–1.03, contribution percentages =

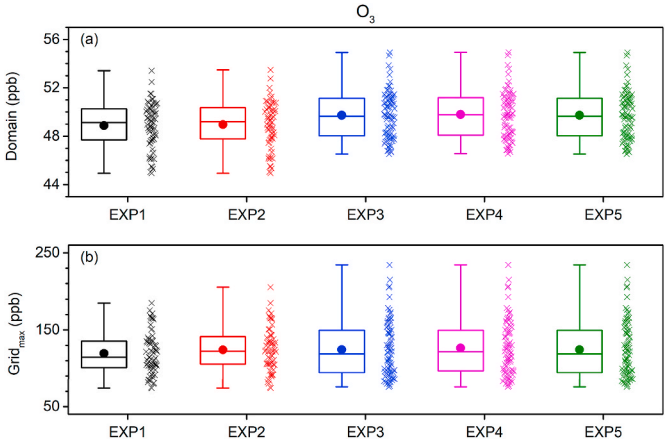

Fig. 4. Monthly (a) domain-averaged and (b) grid maximum O_3 concentrations (cross marks, unit: ppb) excluding data points lower than 40 ppb in WUS. The definitions of experiments are described in the main texts. Each box-whisker plot includes the information of the minimum (lower end), the first quartile (lower bound of the box), the median (line inside the box), the third quartile (upper bound of the box), and the maximum (upper end). Mean values are shown in filled circles.

0.2–50.6%) during the summer seasons regarding the maximum O_3 values at the grid-cell level (Fig. S11). The slight increases of O_3 concentrations in a warmer future climate result in a few more exceedance days compared to the present climate. The simulated exceedance days by O_3 change from 2 days/year to 5 days/year with the FINN3D_RCP85 emissions, even though the total exceedance days decrease from 208 days/year in EXP1 and 210 days/year in EXP2 to 194 days/year in EXP3 and 199 days/year in EXP4 (Table 1). Unaccounted small wildfire contributions to the O_3 concentrations by the EFM emissions are suggested to cause unchanged exceedance days simulated in EXP5 with respect to EXP3.

3.3. Uncertainty of air quality projections due to wildfire emissions

Results from EXP4 and EXP5 exhibit large variations in projecting future air pollutant concentrations. Such variations are attributed to the projections of the wildfire emissions since all climate, ICBC, and sectoral emission inputs excluding wildfires are identical between the two experiments. Here we select four grid cells (Fig. S12) to investigate how FINN3D_RCP85 and EFM wildfire emissions influence the city-scale $PM_{2.5}$ levels in WUS. We find that daily $PM_{2.5}$ concentrations vary substantially between the two wildfire emissions during June 2051 (Fig. S13). While $PM_{2.5}$ variations in EXP4 and EXP5 generally agree with each other at the southern California location (Fig. 13(b)), high episodic $PM_{2.5}$ increases with the FINN3D_RCP85 emissions are projected at the northern California location on June 5, 2051 (61 μg/m^3, R_{grid} = 24, and 96% for the contribution ratio) and during June 24–26, 2051 (2–17 μg/m^3, R_{grid} = 1–7, and 38–87% for the contribution ratios) whereas the EFM emissions induce negligible $PM_{2.5}$ changes at this location (Fig. 13(a)). On the contrary, large wildfires observed at the Colorado and Arizona locations during June 2001 lead to high EFM wildfire emission projections in June 2051, causing the largest $PM_{2.5}$ increase of 54 μg/m^3 (R_{grid} = 28 and 97% for the contribution ratio) on June 5, 2051 (Fig. 13(c)) at the Colorado location and 124 μg/m^3 (R_{grid} = 32 and 97% for the contribution ratio) at the Arizona location on June 1, 2051 (Fig. 13(d)). These results demonstrate how different wildfire emission projections considerably influence the simulated air pollutant concentrations in the future. In this study, the FINN3D_RCP85 emissions include both small and large wildfires but they are projected according to the 2005 USEPA emission profiles. The lack of the temporal changes between years can cause biases in air pollutant estimates. On the other hand, the EFM emissions are a high-resolution emission dataset projected at the locations where large fires occur in the present climate. Nevertheless, an important caveat of the EFM emissions lies in the missing small wildfires, which can contribute to the total fire emissions as much as large wildfires when the burning period becomes longer. Future simulations are suggested to consider both large and small wildfire events with varying annual wildfire temporal profiles to improve the estimates of wildfire impacts on air quality either at city or regional scales.

4. Conclusion

This study combines observations and model simulation results to investigate the evolution of wildfire impacts on air pollutants in WUS from the present climate to the future climate. To our knowledge, this is the first study to evaluate future wildfire impacts on air toxics that have high health risk potentials in this region. We find that smaller pollutant concentration changes but higher contribution ratios by wildfires are projected under the RCP8.5 scenario compared to that during the present climate. This suggests an increasing role of wildfires in altering the pollutant concentrations, which in turn affect human health as more annual exceedance days are projected. In addition, our simulations with high spatial and temporal resolutions enable the evaluations of wildfire impacts on air pollutants at both regional and city levels. While small wildfire impacts on regional (domain-averaged) air pollutant concentrations are simulated, the city-scale pollutant concentrations rise substantially by wildfires. Since human activities expand rapidly from urban to rural areas in recent years, wildfire impacts at the wildland-urban interface (Radeloff et al., 2005) become an emerging concern. Inappropriate coarse grid-resolution simulations or analyses with domain-averaged values may induce large biases in underestimating wildfire impacts on air quality at the wildland-urban interface. We therefore suggest that future wildfire studies should consider conducting simulations at city or appropriate regional scales, which are crucial for decision-making processes on air quality, public health, and wildfire management.

Author statement

Cheng-En Yang: Investigation, Methodology, Data curation, Formal analysis, Software, Visualization, Writing – original draft preparation. ***Joshua Fu***: Conceptualization, Supervision, Project administration, Writing – review & editing, Funding acquisition; ***Yang Liu***: Conceptualization, Supervision, Project administration, Writing – review & editing, Funding acquisition. ***Xinyi Dong***: Investigation, Data curation, Software, Writing – review & editing. ***Yongqiang Liu***: Investigation, Methodology, Data curation, Formal analysis, Writing – review & editing.

Declaration of competing interest

The authors declare that they have no known competing financial interests or personal relationships that could have appeared to influence the work reported in this paper.

Acknowledgements

This study was supported by the U.S. EPA Science to Achieve Results (STAR) Grant R835869. This research used resources of the Oak Ridge Leadership Computing Facility at the Oak Ridge National Laboratory, which is supported by the Office of Science of the U.S. Department of Energy under Contract No. DE-AC05-00OR22725.

Appendix A. Supplementary data

Supplementary data to this article can be found online at https://doi.org/10.1016/j.envpol.2022.119213.

References

Air Sciences Inc, 2005. 2002 Fire Emission Inventory for the WRAP Region – Phase II, Prepared for the Western Governors Association/Western Regional Air Partnership (Denver, CO, USA.

Allen, D.J., Pickering, K.E., Duncan, B., Damon, M., 2010. Impact of lightning NO emissions on North American photochemistry as determined using the Global Modeling Initiative (GMI) model. J. Geophys. Res. Atmos. 115 https://doi.org/10.1029/2010JD014062.

Allen, D.J., Pickering, K.E., Pinder, R.W., Henderson, B.H., Appel, K.W., Prados, A., 2012. Impact of lightning-NO on eastern United States photochemistry during the summer of 2006 as determined using the CMAQ model. Atmos. Chem. Phys. 12, 1737–1758. https://doi.org/10.5194/acp-12-1737-2012.

Alves, C.A., Vicente, A., Monteiro, C., Gonçalves, C., Evtyugina, M., Pio, C., 2011. Emission of trace gases and organic components in smoke particles from a wildfire in a mixed-evergreen forest in Portugal. Sci. Total Environ. 409, 1466–1475. https://doi.org/10.1016/j.scitotenv.2010.12.025.

Andreae, M.O., Merlet, P., 2001. Emission of trace gases and aerosols from biomass burning. Global Biogeochem. Cycles 15, 955–966. https://doi.org/10.1029/2000GB001382.

Appel, K.W., Napelenok, S.L., Foley, K.M., Pye, H.O.T., Hogrefe, C., Luecken, D.J., Bash, J.O., Roselle, S.J., Pleim, J.E., Foroutan, H., Hutzell, W.T., Pouliot, G.A., Sarwar, G., Fahey, K.M., Gantt, B., Gilliam, R.C., Heath, N.K., Kang, D., Mathur, R., Schwede, D.B., Spero, T.L., Wong, D.C., Young, J.O., 2017. Description and evaluation of the Community Multiscale Air Quality (CMAQ) modeling system version 5.1. Geosci. Model Dev 10, 1703–1732. https://doi.org/10.5194/gmd-10-1703-2017.

Binkowski, F.S., Arunachalam, S., Adelman, Z., Pinto, J.P., 2007. Examining photolysis rates with a prototype online photolysis module in CMAQ. J. Appl. Meteorol. Climatol. 46, 1252–1256. https://doi.org/10.1175/JAM2531.1.

Booze, T.F., Reinhardt, T.E., Quiring, S.J., Ottmar, R.D., 2004. A screening-level assessment of the health risks of chronic smoke exposure for wildland firefighters. J. Occup. Environ. Hyg. 1, 296–305. https://doi.org/10.1080/15459620490442500.

Boylan, J.W., Russell, A.G., 2006. PM and light extinction model performance metrics, goals, and criteria for three-dimensional air quality models. Atmos. Environ. 40, 4946–4959. https://doi.org/10.1016/j.atmosenv.2005.09.087.

Byun, D., Schere, K.L., 2006. Review of the governing equations, computational algorithms, and other components of the models-3 community Multiscale Air quality (CMAQ) modeling system. Appl. Mech. Rev. 59, 51. https://doi.org/10.1115/1.2128636.

Carlton, A.G., Bhave, P.V., Napelenok, S.L., Edney, E.O., Sarwar, G., Pinder, R.W., Pouliot, G.A., Houyoux, M., 2010. Model representation of secondary organic aerosol in CMAQv4.7. Environ. Sci. Technol. 44, 8553–8560. https://doi.org/10.1021/es100636q.

Cayan, D.R., Das, T., Pierce, D.W., Barnett, T.P., Tyree, M., Gershunov, A., 2010. Future dryness in the southwest US and the hydrology of the early 21st century drought. Proc. Natl. Acad. Sci. U.S.A. 107, 21271–21276. https://doi.org/10.1073/pnas.0912391107.

Chylek, P., Dubey, M., Hengartner, N., Klett, J., 2017. Observed and projected precipitation changes over the nine US climate regions. Atmosphere 8, 207. https://doi.org/10.3390/atmos8110207.

Cohen, J.D., Deeming, J.E., 1985. The National Fire-Danger Rating System: Basic Equations, Gen. Tech. Rep. PSW-GTR-82. U.S. Department of Agriculture, Forest Service, Pacific Southwest Forest and Range Experiment Station, Berkeley, CA.

Colella, P., Woodward, P.R., 1984. The piecewise parabolic method (PPM) for gas-dynamical simulations. J. Comput. Phys. 54, 174–201. https://doi.org/10.1016/0021-9991(84)90143-8.

Dennison, P.E., Brewer, S.C., Arnold, J.D., Moritz, M.A., 2014. Large wildfire trends in the western United States, 1984–2011. Geophys. Res. Lett. 41, 2928–2933. https://doi.org/10.1002/2014GL059576.

Dominici, F., Zanobetti, A., Schwartz, J., Braun, D., Sabath, B., Wu, X., 2022. Assessing adverse health effects of long-term exposure to low levels of ambient air pollution: implementation of causal inference methods. Res. Rep. Health Eff. Inst. 211, 2022.

Emmons, L.K., Walters, S., Hess, P.G., Lamarque, J.-F., Pfister, G.G., Fillmore, D., Granier, C., Guenther, A., Kinnison, D., Laepple, T., Orlando, J., Tie, X., Tyndall, G., Wiedinmyer, C., Baughcum, S.L., Kloster, S., 2010. Description and evaluation of the model for ozone and related chemical Tracers, version 4 (MOZART-4). Geosci. Model Dev 3, 43–67. https://doi.org/10.5194/gmd-3-43-2010.

Fahey, K.M., Carlton, A.G., Pye, H.O.T., Baek, J., Hutzell, W.T., Stanier, C.O., Baker, K.R., Appel, K.W., Jaoui, M., Offenberg, J.H., 2017. A framework for expanding aqueous chemistry in the Community Multiscale Air Quality (CMAQ) model version 5.1. Geosci. Model Dev 10, 1587–1605. https://doi.org/10.5194/gmd-10-1587-2017.

Ford, B., Val Martin, M., Zelasky, S.E., Fischer, E.V., Anenberg, S.C., Heald, C.L., Pierce, J.R., 2018. Future fire impacts on smoke concentrations, visibility, and health in the contiguous United States. GeoHealth 2, 229–247. https://doi.org/10.1029/2018GH000144.

Fu, J.S., Hsu, N.C., Gao, Y., Huang, K., Li, C., Lin, N.-H., Tsay, S.-C., 2012. Evaluating the influences of biomass burning during 2006 BASE-ASIA: a regional chemical transport modeling. Atmos. Chem. Phys. 12, 3837–3855. https://doi.org/10.5194/acp-12-3837-2012.

Gao, Y., Fu, J.S., Drake, J.B., Lamarque, J.-F., Liu, Y., 2013. The impact of emission and climate change on ozone in the United States under representative concentration pathways (RCPs). Atmos. Chem. Phys. 13, 9607–9621. https://doi.org/10.5194/acp-13-9607-2013.

Gao, Y., Fu, J.S., Drake, J.B., Liu, Y., Lamarque, J.-F., 2012. Projected changes of extreme weather events in the eastern United States based on a high resolution climate modeling system. Environ. Res. Lett. 7, 044025 https://doi.org/10.1088/1748-9326/7/4/044025.

Gao, Y., Leung, L.R., Lu, J., Liu, Y., Huang, M., Qian, Y., 2014. Robust spring drying in the southwestern U.S. and seasonal migration of wet/dry patterns in a warmer climate. Geophys. Res. Lett. 41, 1745–1751. https://doi.org/10.1002/2014GL059562.

Giglio, L., Randerson, J.T., van der Werf, G.R., 2013. Analysis of daily, monthly, and annual burned area using the fourth-generation global fire emissions database (GFED4). J. Geophys. Res. Biogeosciences 118, 317–328. https://doi.org/10.1002/jgrg.20042.

Goss, M., Swain, D.L., Abatzoglou, J.T., Sarhadi, A., Kolden, C.A., Williams, A.P., Diffenbaugh, N.S., 2020. Climate change is increasing the likelihood of extreme autumn wildfire conditions across California. Environ. Res. Lett. 15, 094016 https://doi.org/10.1088/1748-9326/ab83a7.

Higuera, P.E., Abatzoglou, J.T., 2021. Record-setting climate enabled the extraordinary 2020 fire season in the western United States. Global Change Biol. 27, 1–2. https://doi.org/10.1111/gcb.15388.

Holden, Z.A., Swanson, A., Luce, C.H., Jolly, W.M., Maneta, M., Oyler, J.W., Warren, D. A., Parsons, R., Affleck, D., 2018. Decreasing fire season precipitation increased recent western US forest wildfire activity. Proc. Natl. Acad. Sci. Unit. States Am. 115, E8349–E8357. https://doi.org/10.1073/pnas.1802316115.

IPCC, 2021. Summary for policymakers. In: Masson-Delmotte, V., Zhai, P., Pirani, A., Connors, S.L., Péan, C., Berger, S., Caud, N., Chen, Y., Goldfarb, L., Gomis, M.I., Huang, M., Leitzell, K., Lonnoy, E., Matthews, J.B.R., Maycock, T.K., Waterfield, T., Yelekçi, R., Yu, R., Zhou, B. (Eds.), Climate Change 2021: the Physical Science Basis. Contribution of Working Group I to the Sixth Assessment Report of the Intergovernmental Panel on Climate Change. Cambridge Univ. Press, UK.

IPCC, 2014. Climate Change 2014: Synthesis Report, Contribution of Working Groups I, II and III to the Fifth Assessment Report of the Intergovernmental Panel on Climate Change. IPCC, Geneva, Switzerland.

Jaffe, D.A., Hafner, W., Chand, D., Westerling, A., Spracklen, D.V., 2008. Interannual variations in $PM_{2.5}$ due to wildfires in the western United States. Environ. Sci. Technol. 42, 2812–2818. https://doi.org/10.1021/es702755v.

Jaffe, D.A., Wigder, N.L., 2012. Ozone production from wildfires: a critical review. Atmos. Environ. 51, 1–10. https://doi.org/10.1016/j.atmosenv.2011.11.063.

Jaffe, D.A., Zhang, L., 2017. Meteorological anomalies lead to elevated O_3 in the western U.S. in June 2015. Geophys. Res. Lett. 44, 1990–1997. https://doi.org/10.1002/2016GL072010.

Knorr, W., Dentener, F., Lamarque, J.-F., Jiang, L., Arneth, A., 2017. Wildfire air pollution hazard during the 21st century. Atmos. Chem. Phys. 17, 9223–9236. https://doi.org/10.5194/acp-17-9223-2017.

Lamarque, J.-F., Emmons, L.K., Hess, P.G., Kinnison, D.E., Tilmes, S., Vitt, F., Heald, C.L., Holland, E.A., Lauritzen, P.H., Neu, J., Orlando, J.J., Rasch, P.J., Tyndall, G.K., 2012. CAM-chem: description and evaluation of interactive atmospheric chemistry in the Community Earth System Model. Geosci. Model Dev. 5, 369–411. https://doi.org/10.5194/gmd-5-369-2012.

Lamarque, J.-F., Kiehl, J.T., Hess, P.G., Collins, W.D., Emmons, L.K., Ginoux, P., Luo, C., Tie, X.X., 2005. Response of a coupled chemistry-climate model to changes in aerosol emissions: global impact on the hydrological cycle and the tropospheric burdens of OH, ozone, and NOx. Geophys. Res. Lett. 32, L16809. https://doi.org/10.1029/2005GL023419.

Littell, J.S., McKenzie, D., Peterson, D.L., Westerling, A.L., 2009. Climate and wildfire area burned in western U.S. ecoprovinces, 1916–2003. Ecol. Appl. 19, 1003–1021. https://doi.org/10.1890/07-1183.1.

Liu, J.C., Mickley, L.J., Sulprizio, M.P., Dominici, F., Yue, X., Ebisu, K., Anderson, G.B., Khan, R.F.A., Bravo, M.A., Bell, M.L., 2016. Particulate air pollution from wildfires in the Western US under climate change. Clim. Change 138, 655–666. https://doi.org/10.1007/s10584-016-1762-6.

Liu, J.C., Pereira, G., Uhl, S.A., Bravo, M.A., Bell, M.L., 2015. A systematic review of the physical health impacts from non-occupational exposure to wildfire smoke. Environ. Res. 136, 120–132. https://doi.org/10.1016/j.envres.2014.10.015.

Liu, Y., Goodrick, S., Heilman, W., 2014a. Wildland fire emissions, carbon, and climate: wildfire–climate interactions. For. Ecol. Manag., Wildland fire emissions, carbon, and climate: Science overview and knowledge needs 317, 80–96. https://doi.org/10.1016/j.foreco.2013.02.020.

Liu, Y., Goodrick, S., Stanturf, J., 2013. Future U.S. wildfire potential trends projected using a dynamically downscaled climate change scenario. For. Ecol. Manag. 294, 120–135. https://doi.org/10.1016/j.foreco.2012.06.049.

Liu, Y., Goodrick, S., Stanturf, J., Tian, H., 2014b. Impacts of Mega-Fire on Large U.S. Urban Area Air Quality under Changing Climate and Fuels, JFSP Project 11-1-7-2. https://www.firescience.gov/projects/11-1-7-2/project/11-1-7-2_final_report.pdf.

Liu, Yongqiang, Liu, Yang, Fu, J., Yang, C.-E., Dong, X., Tian, H., Tao, B., Yang, J., Wang, Y., Zou, Y., Ke, Z., 2021. Projection of future wildfire emissions in western USA under climate change: contributions from changes in wildfire, fuel loading and fuel moisture. Int. J. Wildland Fire 31, 1–13. https://doi.org/10.1071/WF20190.

Marlon, J.R., Bartlein, P.J., Gavin, D.G., Long, C.J., Anderson, R.S., Briles, C.E., Brown, K. J., Colombaroli, D., Hallett, D.J., Power, M.J., Scharf, E.A., Walsh, M.K., 2012. Long-term perspective on wildfires in the western USA. Proc. Natl. Acad. Sci. U.S.A. 109, E535–E543. https://doi.org/10.1073/pnas.1112839109.

Myhre, G., Shindell, D., Bréon, F.-M., Collins, W., Fuglestvedt, J., Huang, J., Koch, D., Lamarque, J.-F., Lee, D., Mendoza, B., Nakajima, T., Robock, A., Stephens, G., Takemura, T., Zhang, H., 2013. Anthropogenic and natural radiative forcing. In: Stocker, T.F., Qin, D., Plattner, G.-K., Tignor, M., Allen, S.K., Boschung, J., Nauels, A., Xia, Y., Bex, V., Midgley, P.M. (Eds.), Climate Change 2013: the Physical Science Basis. Contribution of Working Group I to the Fifth Assessment Report of the Intergovernmental Panel on Climate Change. Cambridge University Press, Cambridge, United Kingdom and New York, NY, USA, pp. 659–740. https://doi.org/10.1017/CBO9781107415324.018.

Na, K., Cocker, D.R., 2008. Fine organic particle, formaldehyde, acetaldehyde concentrations under and after the influence of fire activity in the atmosphere of Riverside, California. Environ. Res. 108, 7–14. https://doi.org/10.1016/j.envres.2008.04.004.

National Primary and Secondary Ambient Air Quality Standards, 2021, 40 C.F.R § 50. https://www.ecfr.gov/current/title-40/chapter-I/subchapter-C/part-50.

Neale, R.B., Richter, J.H., Conley, A.J., Park, S., Lauritzen, P.H., Gettelman, A., Williamson, D.L., Rasch, P.J., Vavrus, S.J., Taylor, M.A., Collins, W.D., Zhang, M., Lin, S.-J., 2010. Description of the NCAR Community Atmosphere Model (CAM4.0) (No. Tech. Rep. NCAR/TN-485+STR). National Center for Atmospheric Research, Boulder, CO, USA.

Nolte, C.G., Spero, T.L., Bowden, J.H., Mallard, M.S., Dolwick, P.D., 2018. The potential effects of climate change on air quality across the conterminous US at 2030 under three Representative Concentration Pathways. Atmos. Chem. Phys. 18, 15471–15489. https://doi.org/10.5194/acp-18-15471-2018.

O'Dell, K., Ford, B., Fischer, E.V., Pierce, J.R., 2019. Contribution of wildland-fire smoke to US $PM_{2.5}$ and its influence on recent trends. Environ. Sci. Technol. 53, 1797–1804. https://doi.org/10.1021/acs.est.8b05430.

OEHHA, 2008. Appendix D. Individual Acute, 8-hour, and Chronic Reference Exposure Level Summaries. TSD for Noncancer RELs.

Otte, T.L., Pleim, J.E., 2010. The Meteorology-Chemistry Interface Processor (MCIP) for the CMAQ modeling system: updates through MCIPv3.4.1. Geosci. Model Dev 3, 243–256. https://doi.org/10.5194/gmd-3-243-2010.

Pfister, G.G., Wiedinmyer, C., Emmons, L.K., 2008. Impacts of the fall 2007 California wildfires on surface ozone: integrating local observations with global model

simulations. Geophys. Res. Lett. 35, L19814. https://doi.org/10.1029/2008GL034747.
Pleim, J.E., 2007. A combined local and nonlocal closure model for the atmospheric boundary layer. Part I: model description and testing. J. Appl. Meteorol. Climatol. 46, 1383–1395. https://doi.org/10.1175/JAM2539.1.
Pye, H.O.T., Pouliot, G.A., 2012. Modeling the role of alkanes, polycyclic aromatic hydrocarbons, and their oligomers in secondary organic aerosol formation. Environ. Sci. Technol. 46, 6041–6047. https://doi.org/10.1021/es300409w.
Radeloff, V.C., Hammer, R.B., Stewart, S.I., Fried, J.S., Holcomb, S.S., McKeefry, J.F., 2005. The wildland–urban interface in the United States. Ecol. Appl. 15, 799–805. https://doi.org/10.1890/04-1413.
Reinhardt, T.E., Ottmar, R.D., 2004. Baseline measurements of smoke exposure among wildland firefighters. J. Occup. Environ. Hyg. 1, 593–606. https://doi.org/10.1080/15459620490490101.
Reisen, F., Duran, S.M., Flannigan, M., Elliott, C., Rideout, K., Reisen, F., Duran, S.M., Flannigan, M., Elliott, C., Rideout, K., 2015. Wildfire smoke and public health risk. Int. J. Wildland Fire 24, 1029–1044. https://doi.org/10.1071/WF15034.
Riahi, K., Rao, S., Krey, V., Cho, C., Chirkov, V., Fischer, G., Kindermann, G., Nakicenovic, N., Rafaj, P., 2011. Rcp 8.5—a scenario of comparatively high greenhouse gas emissions. Clim. Change 109, 33–57. https://doi.org/10.1007/s10584-011-0149-y.
Short, K., 2013. Sources and implications of bias and uncertainty in a century of us wildfire activity data. Int. J. Wildland Fire 24, 883–891.
Simon, H., Bhave, P.V., 2012. Simulating the degree of oxidation in atmospheric organic particles. Environ. Sci. Technol. 46, 331–339. https://doi.org/10.1021/es202361w.
Skamarock, W.C., Klemp, J.B., 2008. A time-split nonhydrostatic atmospheric model for weather research and forecasting applications. J. Comput. Phys. 227, 3465–3485. https://doi.org/10.1016/j.jcp.2007.01.037.
Spracklen, D.V., Mickley, L.J., Logan, J.A., Hudman, R.C., Yevich, R., Flannigan, M.D., Westerling, A.L., 2009. Impacts of climate change from 2000 to 2050 on wildfire activity and carbonaceous aerosol concentrations in the western United States. J. Geophys. Res. 114, D20301. https://doi.org/10.1029/2008JD010966.
Stowell, J.D., Geng, G., Saikawa, E., Chang, H.H., Fu, J., Yang, C.-E., Zhu, Q., Liu, Y., Strickland, M.J., 2019. Associations of wildfire smoke $PM_{2.5}$ exposure with cardiorespiratory events in Colorado 2011–2014. Environ. Int. 133, 105151. https://doi.org/10.1016/j.envint.2019.105151.
Tai, E., Jimenez, M., Nopmongcol, O., Wilson, G., Mansell, G., Koo, B., Yarwood, G., 2008. Boundary Conditions and Fire Emissions Modeling (Final Report No. 582- 07-84005-FY08-10). ENVIRON International Corporation., Novato, CA.
Taylor, K.E., Stouffer, R.J., Meehl, G.A., 2012. An overview of CMIP5 and the experiment design. Bull. Am. Meteorol. Soc. 93, 485–498. https://doi.org/10.1175/BAMS-D-11-00094.1.
Tian, H., Chen, G., Liu, M., Zhang, C., Sun, G., Lu, C., Xu, X., Ren, W., Pan, S., Chappelka, A., 2010. Model estimates of net primary productivity, evapotranspiration, and water use efficiency in the terrestrial ecosystems of the southern United States during 1895–2007. For. Ecol. Manag. 259, 1311–1327. https://doi.org/10.1016/j.foreco.2009.10.009.
UNC Institute for the Environment, 2009. SMOKE v2.6 User's Manual. The University of North Carolina at Chapel, Chapel Hill, NC, USA.
Urbanski, S.P., 2014. Wildland fire emissions, carbon, and climate: emission factors. For. Ecol. Manag. 317, 51–60. https://doi.org/10.1016/j.foreco.2013.05.045.
Urbanski, S.P., Hao, W.M., Baker, S., 2008. Chemical composition of wildland fire emissions. In: Bytnerowicz, A., Arbaugh, M., Riebau, A., Andersen, C. (Eds.), Wildland Fires and Air Pollution, Developments in Environmental Science. Elservier, pp. 79–107. https://doi.org/10.1016/S1474-8177(08)00004-1.
Urbanski, S.P., Hao, W.M., Nordgren, B., 2011. The wildland fire emission inventory: western United States emission estimates and an evaluation of uncertainty. Atmos. Chem. Phys. 11, 12973–13000. https://doi.org/10.5194/acp-11-12973-2011.
Val Martin, M., Heald, C.L., Lamarque, J.-F., Tilmes, S., Emmons, L.K., Schichtel, B.A., 2015. How emissions, climate, and land use change will impact mid-century air quality over the United States: a focus on effects at national parks. Atmos. Chem. Phys. 15, 2805–2823. https://doi.org/10.5194/acp-15-2805-2015.
Veira, A., Lasslop, G., Kloster, S., 2016. Wildfires in a warmer climate: emission fluxes, emission heights, and black carbon concentrations in 2090–2099. J. Geophys. Res. Atmos. 121, 3195–3223. https://doi.org/10.1002/2015JD024142.
Wiedinmyer, C., Akagi, S.K., Yokelson, R.J., Emmons, L.K., Al-Saadi, J.A., Orlando, J.J., Soja, A.J., 2011. The Fire INventory from NCAR (FINN): a high resolution global model to estimate the emissions from open burning. Geosci. Model Dev. 4, 625–641. https://doi.org/10.5194/gmd-4-625-2011.
Wiedinmyer, C., Neff, J.C., 2007. Estimates of CO_2 from fires in the United States: implications for carbon management. Carbon Bal. Manag. 2, 10. https://doi.org/10.1186/1750-0680-2-10.
Wiedinmyer, C., Quayle, B., Geron, C., Belote, A., McKenzie, D., Zhang, X., O'Neill, S., Wynne, K.K., 2006. Estimating emissions from fires in North America for air quality modeling. Atmos. Environ. 40, 3419–3432. https://doi.org/10.1016/j.atmosenv.2006.02.010.
Wilkins, J.L., Pouliot, G., Foley, K., Appel, W., Pierce, T., 2018. The impact of US wildland fires on ozone and particulate matter: a comparison of measurements and CMAQ model predictions from 2008 to 2012. Int. J. Wildland Fire 27, 684–698.
Williams, A.P., Abatzoglou, J.T., Gershunov, A., Guzman-Morales, J., Bishop, D.A., Balch, J.K., Lettenmaier, D.P., 2019. Observed impacts of anthropogenic climate change on wildfire in California. Earth's Future 7, 892–910. https://doi.org/10.1029/2019EF001210.
Wong, D.C., Pleim, J., Mathur, R., Binkowski, F., Otte, T., Gilliam, R., Pouliot, G., Xiu, A., Young, J.O., Kang, D., 2012. WRF-CMAQ two-way coupled system with aerosol feedback: software development and preliminary results. Geosci. Model Dev. 5, 299–312. https://doi.org/10.5194/gmd-5-299-2012.
World Health Organization, 2010. WHO Guidelines for Indoor Air Quality: Selected Pollutants. World Health Organization. Regional Office for Europe. https://apps.who.int/iris/handle/10665/260127.
Xing, J., Pleim, J., Mathur, R., Pouliot, G., Hogrefe, C., Gan, C.-M., Wei, C., 2013. Historical gaseous and primary aerosol emissions in the United States from 1990 to 2010. Atmos. Chem. Phys. 13, 7531–7549. https://doi.org/10.5194/acp-13-7531-2013.
Yue, X., Mickley, L.J., Logan, J.A., Kaplan, J.O., 2013. Ensemble projections of wildfire activity and carbonaceous aerosol concentrations over the western United States in the mid-21st century. Atmos. Environ. 77, 767–780. https://doi.org/10.1016/j.atmosenv.2013.06.003.